JOURNAL OF MATERIALS SCIENCE **39** (2004) 3941 – 3947

Magnetic properties and thermal stability of CoFeNi-based amorphous films

A. KÄUFLER, Y. LUO, K. SAMWER
Physikalisches Institut, Universität Göttingen, Bunsenstr. 9, D-37073 Göttingen, Germany
E-mail: yluo@gwdg.de

CoNiFe-based amorphous films were magnetron-sputtered to investigate their structural and magnetic properties, including annealing-induced effects and interfacial influence from additional layers of Ta and Cu. The amorphous structure was confirmed by diffraction experiments. The magnetic measurements showed a well-defined uniaxial anisotropy in plane, arising possibly from atom oblique incidence effects competing with the stray field of the magnetron. The anisotropy could be influenced by using a Ta buffer layer, though the interfacial reaction gives rise to a dead layer. A coercive force H_c of 1–2 Oe and a magnetization of 680 emu/cm^3 were measured at room temperature; properties which show promise for application in magnetotunneling junction devices. Thermal analyses showed a two-stage crystallization behavior, which started at 400°C and ended at about 600°C. The Curie temperature of the amorphous phase was estimated to be about 440°C.

1. Introduction

Following the discovery of giant magnetoresistance (GMR) and tunneling magnetoresistance (TMR) successively in relevant magnetic layered systems[1, 2], a large number of investigations have been made both theoretically and experimentally for understanding their spin dependent transport behaviors. Generally, a TMR junction consists of a soft and a hard magnetic layer as two electrodes separated by a thin isolator layer as an electrical barrier. A GMR spin valve has a similar structure, but two magnetic layers are separated by a metallic layer. The resistance changes its value in these structures when the soft magnetic detection layer is switched by applying an external magnetic field. Usually, the TMR effect of a junction structure is larger than the GMR effect of a spin-valve structure and is very promising for applications such as low-field sensors and magnetoresistance random access memories [3]. For memory applications, for example, writing a bit information is performed by switching the detection layer, where the switching field is induced by a current pulse in the word line consisting of a Cu layer separated from the TMR storage element by an isolator layer. To lower power consumption and access time, a small critical switching field is desired. On the other hand, high density memories imply reduction in the lateral size of junction devices, leading to increase of the demagnetizing effect [4] which can be compensated by using very thin magnetic layers.

In most case, permalloy $Ni_{81}Fe_{19}$ is chosen as the detection layer since it possesses a low crystalline anisotropy and a zero magnetostriction and hence a rather low coercivity H_c. Furthermore, permalloy reveals a sufficiently high spin polarization essential for a high TMR effect. Alternatively, we have attempted to design TMR junctions using CoFeNi-based amorphous materials. Without grain boundaries for pinning of the domain walls, these materials exhibit excellent soft magnetic properties. Also a sufficient saturation magnetization [5] and a zero magnetostriction should be favorable for magnetoelectronic devices. Indeed, our initial results obtained from the junction structure containing a thin $Co_{64}Fe_5Ni_5Si_{13}B_{13}$ film as detection layer showed a TMR effect of about 22% at room temperature [6].

This paper deals with the structural and magnetic properties of $Co_{64}Fe_5Ni_5Si_{13}B_{13}$ (CoFeNiSiB) amorphous films in more detail, involving annealing-induced effects and interfacial influences from additional layers Ta and Cu. The additional layers were applied in correspondence with design requirements of the TMR junctions, in which Cu is often used as the capping layer to eliminate the inhomogeneous current effect and Ta as the buffer layer to diminish the interfacial roughness. The interfacial reactions are expected to be quite different due to the opposite sign of the heat of mixing of Cu-Co and Ta-Co systems (note that Co, which comprises 64 at.%, is the major constituent in our amorphous films). The Ta buffer layer lowers interfacial roughness, but interfacial mixing may occur due to a negative heat of mixing and as a result, it leads to a limited dead layer in the samples, as often observed in Ta/NiFe layered structures [7].

2. Experimental details

The samples were sputtered at ambient temperature in a multi-magnetron system with a base pressure

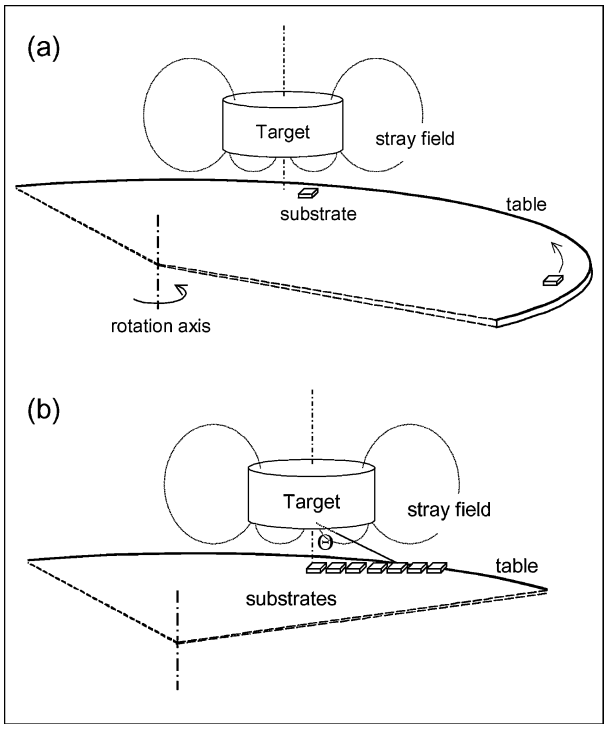

Figure 1 Schematic representation of the magnetron sputtering system: (a) arrangement for moving substrates (used for most of the sample preparations) and (b) arrangement for fixed substrates (used for study the growth-induced magnetic anisotropy).

of 10^{-8} torr and a sputtering pressure of Ar of 3×10^{-3} Torr, where an alloy target of $Co_{64}Fe_5Ni_5Si_{13}B_{13}$ (4 inches) was used for preparation of magnetic amorphous layers. The substrates (10×10 mm^2) were thermally oxidized Si(100) and mounted on a round table (60 cm diameter), which rotates about its central axis and carries the substrates passing the sputtering target (Fig. 1a). The distance between the substrate table and the target was about 40 mm. At this distance, the stray field of the magnetron was measured to be about 150 Oe. Considering the much smaller size of the substrates with respect to the target diameter, we take only the stray field parallel to the substrate moving direction into account, as schematically shown in Fig. 1. Most samples studied here were sputtered in this manner, including sample series 1 (Table I) with varied layer thickness from 2 to 10 nm for CoNiFeSiB. The additional layers of Ta and Cu were sputtered to study their interfacial influence on magnetic properties, especially in the thinnest sample (2 nm).

Additionally, to understand the growth-induced anisotropy mentioned below, the sputter geometric effect was studied here using sample series 2 prepared in another way, where the substrates were fixed beneath the target and arranged one by one in a straight line parallel to the stray field (Fig. 1b). In this way, the mean incidence angle Θ of the incoming atoms to the substrate surface was varied from 25–75°. One should note, at small Θ (<45°) substrates are located just beneath the target and therefore the influence of the stray field should be much larger than that at large Θ. In addition, the different substrate-target distance leads to a variation in deposition rate. Therefore sample series 2 has a thickness ranging from 40 nm for $\Theta = 30°$ to 10 nm for $\Theta = 75°$. Nevertheless, the thickness dependence of magnetic properties measured is insignificant in this range.

TABLE I Two sample series, layered structures and deposition conditions

Series 1	– CoFeNiSiB(t)/Cu(4 nm) – Ta(2 nm)/CoFeNiSiB(t)/Cu(4 nm) – CoFeNiSiB(t)/Ta(2 nm) – Ta(2 nm)/CoFeNiSiB(t)/Ta(2 nm)	with moving substrates (Fig. 1a) and varied thickness (t = 2–10 nm) for amorphous layers
Series 2	– CoFeNiSiB/Ta(2 nm) – Ta(5 nm)/CoFeNiSiB/Ta(2 nm)	with fixed substrates (Fig. 1b) and varied incidence angle Θ

The chemical stoichiometry of the prepared CoFeNiSiB films was determined by electron microprobe to be in accordance with that of the target. The amorphous structure was confirmed by means of X-ray and electron diffraction measurements [8]. To clarify growth-induced anisotropy, surface topography of the films was investigated by scanning tunneling microscopy (STM). Annealing behaviors were analyzed both by differential scanning calorimetry (DSC) and by *in-situ* thermomagnetic experiments with an external magnetic field of 50 Oe. The X-ray and DSC experiments were carried out using relatively thick samples to enhance the measure signals. Magnetization M(H) loops were measured by vibrating sample magnetometer (VSM) and longitudinal magnetooptical Kerr effect (MOKE) with an external field in plane.

3. Results and discussion

Fig. 2 represents an electron diffraction pattern obtained from an as-prepared CoFeNiSiB film. It can be seen that because of the shorter wavelength, the electron diffraction pattern contains more detailed structural information in comparison with X-ray scattering data (see Fig. 3a). As is typical for amorphous structures one sees several halo-like diffuse rings in Fig. 2, where the second ring is split into two subrings with a

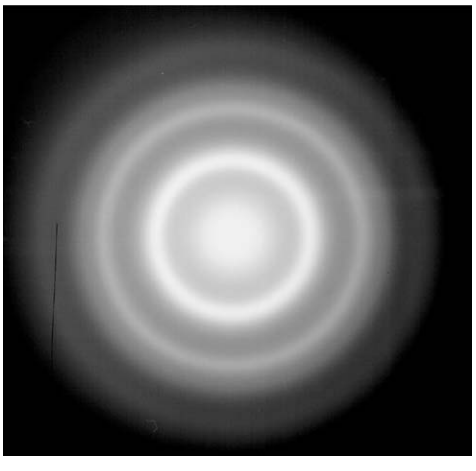

Figure 2 Electron diffraction pattern of a 30 nm CoFeNiSiB film, indicating a typical amorphous structure of metallic glasses. From the full width at half-maximum of the diffraction peak, the radius of short range order was estimated to be about 1.5 nm.

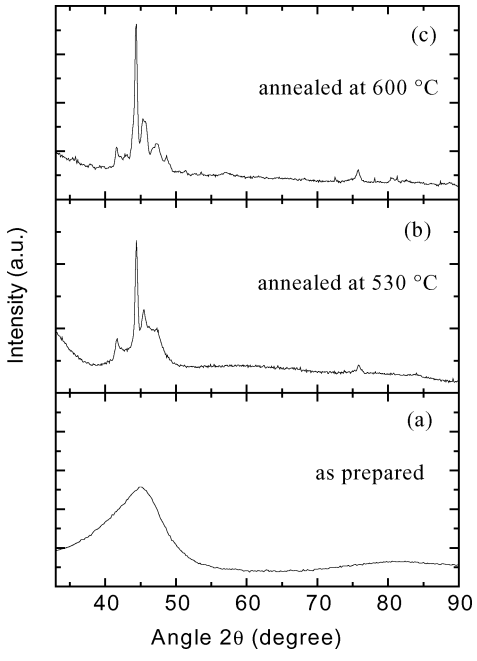

Figure 3 X-ray diffraction patterns measured for a thick CoFeNiSiB film (0.54 μm) before (a) and after annealing at 530°C (b) and 600°C (c) respectively, using Cu K_α radiation.

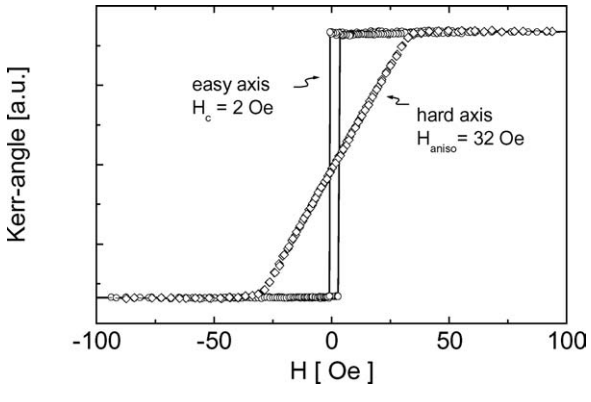

Figure 4 MOKE loop measured from a CoFeNiSiB film (6 nm), showing a well-defined uniaxial anisotropy in-plane with a small coercive field H_c of 2 Oe along the easy axis and an anisotropic field H_{aniso} of 32 Oe along the hard axis.

scattering vector of 0.510 and 0.595 nm^{-1} respectively. The ratios of the scattering vector to that of the first ring (0.310 nm^{-1}) amount to 1.65 and 1.92 in accordance with those measured earlier for the ribbon samples [9]. From the full width at half-maximum of the diffraction peak, the radius of short range order was estimated to be about 1.5 nm.

Fig. 4 shows typical MOKE loops measured in easy and hard axis directions for a sample prepared with moving substrates (Fig. 1a). The result demonstrates a well-defined uniaxial anisotropy with a small coercive field $H_c = 2$ Oe along the easy axis and an anisotropic field $H_{aniso} = 32$ Oe along the hard axis. The given value for H_{aniso} was obtained here as the field on the hard axis loop, where the MOKE signal equals to 90% of its saturation value. The well-defined uniaxial anisotropy and the very small H_c value, which is comparable to that of permalloy, indicate that soft magnetic amorphous CiFeNiSiB thin films are ideal detection layers for TMR-junction applications [6].

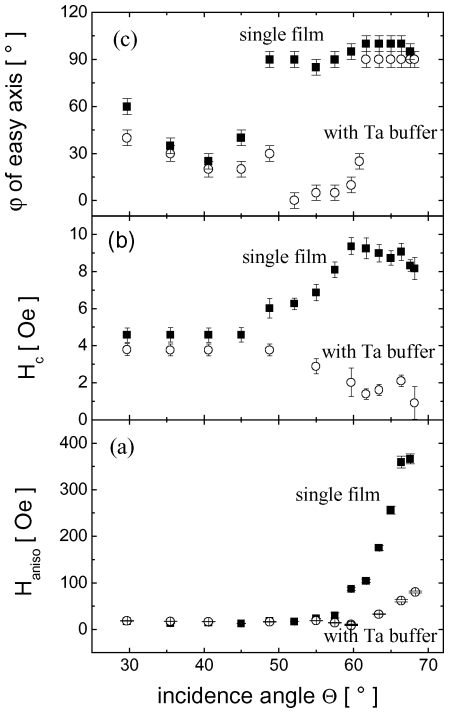

Figure 5 Incidence-angle-dependent magnetic anisotropy characterized by (a) anisotropic field H_{aniso}, (b) coercive field H_c and (c) orientation of the easy axis φ (here φ is the angle with respect to the stray field), including the influence from a Ta buffer layer.

However, the MOKE loop in Fig. 4 indicates an easy axis which is not parallel, but perpendicular to the substrate moving direction (also to the stray field direction). This result suggests that there must be another mechanism which induces magnetic anisotropy in plane and competes with the influence from the stray field. To understand this behavior, magnetic measurements were made for sample series 2 prepared with fixed substrates (Fig. 1b). The results are illustrated in Fig. 5, which indeed show a dependence on the incidence angle Θ. Namely, in the case of $\Theta < 45°$ the samples show an easy axis parallel to the stray field (see Fig. 5c, where φ was defined as the angle between the easy axis and the stray field), indicating that the magnetic anisotropy is induced by an "external" magnetic field. The anisotropic field H_{aniso} is within 20 Oe and the coercive field H_c of about 4 Oe is relatively small (Fig. 5b). With increased Θ, however, the H_{aniso} first slightly changes in size and then drastically increases. At the same time, the easy axis is rotated by 90° in plane (see Fig. 5c). The rotation of the easy axis observed for large Θ suggests a kind of oblique incidence effect which, as discussed below, must be dominant for all the samples prepared with moving substrates.

As is well known, an external magnetic field applied during the film growth induces uniaxial anisotropy in plane with an easy axis parallel to the applied magnetic field. The phenomenon can be attributed to directional pair ordering of magnetic atoms, arising from pseudo dipole-dipole interactions [10]. Usually, by means of a thermal activation the atomic pairs are easily aligned in an external magnetic field [11]. This alignment minimizes the total magnetic energy.

Alternately, the magnetic anisotropy induced by the oblique incidence effect could be connected with

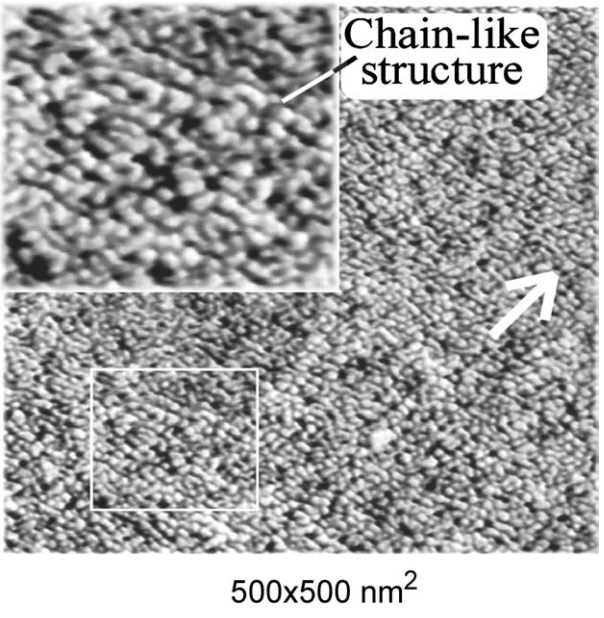

Figure 6 STM image of a CoFeNiSiB film (25 nm), showing a chain-like structure on the film surface. The arrow indicates the atom incidence direction.

topographical anisotropy of the film surface. To investigate this possibility, STM experiments were performed for the samples, which were deposited at large Θ and display an easy axis perpendicular to the stray field. Fig. 6 reveals a typical STM image for these samples. A hillock-like structure like the one here is often observed for amorphous thin films [12, 13]. On more detailed examination however, one sees a chain-like structure perpendicular to the atom incidence direction marked by an arrow (Fig. 6). From the fact, that the easy axis just lies in the chain direction, we can deduce a conclusion that the magnetic anisotropy arises from topographical anisotropy. Like a shape-induced effect, a chain-like structure may cause a surface magnetostatic contribution which determines the direction of the local magnetization in films.

In fact, for the case given in Fig. 1a, the film growth underwent an extensive change of the incidence angle Θ. Possibly, the first sublayer deposited at a large Θ was already influenced by the oblique incidence effect. The local magnetization induced in the sublayer determines the anisotropic behavior in the total film though a stray field of the magnetron exists at small Θ. Obviously, the stray field (maximum 150 Oe) is insufficient to rotate the magnetization direction of the first deposited sublayer, in which the anisotropic field along the hard axis exceeds 300 Oe (see Fig. 5a).

The oblique incidence effect can be influenced by using a Ta buffer layer. As can be seen in Fig. 5, the magnetic anisotropy measured for samples with a Ta buffer layer exhibits a small dependence on Θ, in contrast with the samples without Ta. Also with Ta the critical angle Θ, where the easy axis is rotated by 90°, shifts to a large value (Fig. 5c). H_{aniso} rises slowly with Θ but stays below 80 Oe. In contrast, H_c does not increase any more, but drops down to 1 or 2 Oe for the case of $\Theta > 60°$ (Fig. 5a). The improvement observed here for the samples with Ta can be attributed to the reduced

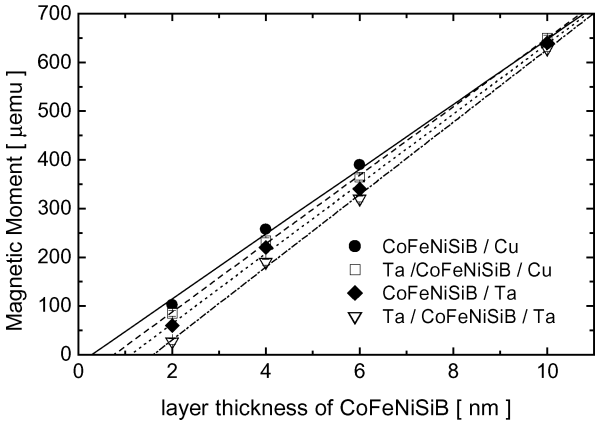

Figure 7 Thickness-dependent magnetic moment measured for samples with additional layers Ta and/or Cu.

layer roughness. A similar result was reported earlier in Ref. [14], where the in-plane magnetic anisotropy induced in permalloy films could be reduced by using a suitable buffer layer.

Fig. 7 demonstrates the magnetic moment M versus the layer thickness (t) of CoFeNiSiB films measured for sample series 1, including the influence from the additional layers Ta and Cu. It can be seen that the magnetic moment M increases linearly with t and achieves about 0.65 emu at $t = 10$ nm. The influence from the additional layers becomes pronounced for small t. A critical layer thickness t_d exists, below which the magnetization of the samples is equal to zero. For this reason, t_d is known as the dead layer thickness. The value of t_d was evaluated by linear extrapolations to the abscissa (Fig. 7) and ranges from 0.2 to 1.6 nm, where the smallest t_d is found in the sample with a Cu capping layer and the largest t_d is measured for a sample with two Ta layers. Because of a negligibly small t_d (0.05 nm) for single films, the observed dead layer thickness for samples with additional layers can be related to interfacial reactions. Accordingly, the largest t_d values for the samples with Ta suggests a strong intermixing at the interfaces possibly due to a negative heat of mixing. Moreover, the sputtering power used for Ta layer preparations was relatively high (1 kW) in comparison to that of Cu (0.5 kW) and CoFeNiSiB (0.1 kW). The higher kinetic energy of the depositing atoms could accelerate the interfacial mixing. In contrast, Cu is immiscible with Co because of a positive heat of mixing and thus the t_d is very small for the samples capped by Cu.

However, the magnetic anisotropy measured for sample series 1 is always nearly independent of the layer thickness of CoFeNiSiB (see Fig. 10), no matter which additional layers were used.

Thermal stability of the amorphous films was studied by DSC analysis. To enhance the heat flow, a thick film of about 0.54 μm was applied with a sample mass of 1.6 mg (without substrate). The DSC curve with a heating rate of 20°C/min was plotted in Fig. 8a, showing two minima near 450 and 570°C, respectively. The result indicates a two-stage crystallization behavior, as observed in most cases for similar CoFeNi-based metallic glasses [9, 15, 16]. The first stage, which starts at a

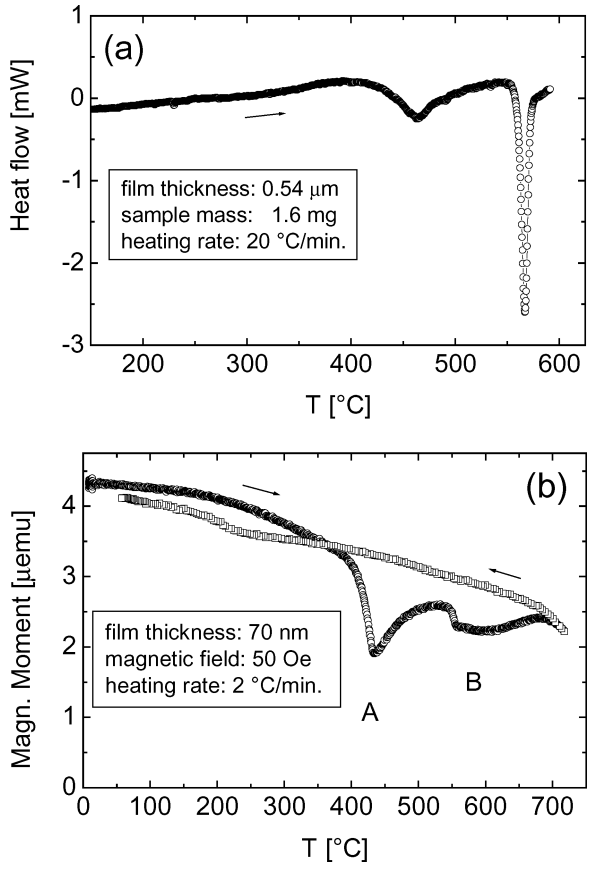

Figure 8 Thermal analyses with (a) DSC and (b) thermomagnetic measurements.

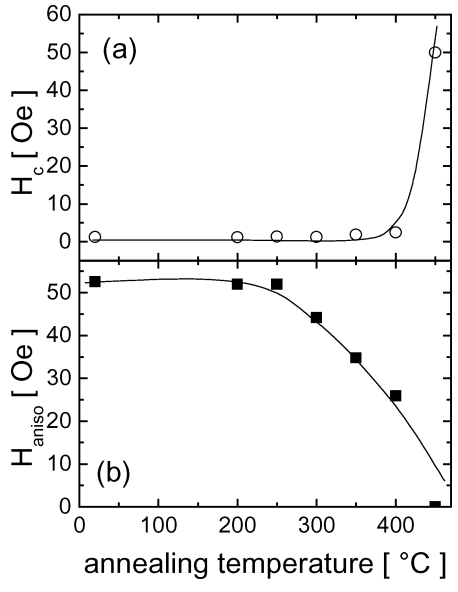

Figure 9 Effect of annealing on the magnetic anisotropy measured for a 90 nm CoFeNiSiB film.

relatively low temperature (400°C) and continues in a broad temperature range ($\Delta T = 150$°C), is associated with nucleation and growth of metastable crystallites within the amorphous matrix. As can be followed in Fig. 3b, the relevant X-ray diffraction pattern shows a phase mixture for this case. The second crystallization stage, which starts at a relatively high temperature (550°C) and continues in a narrow temperature range ($\Delta T = 30$°C), is associated with formation of equilibrium phases. Accordingly, the sample after heating at 600°C exhibits a fully crystalline diffraction pattern (Fig. 3c).

The two-stage crystallization behavior was also manifested by thermomagnetic $M(T)$ measurements, where the magnetic transition of the amorphous phase was observed near 400°C (see Fig. 8b), accompanied with significant decrease in the magnetic moment. Because of the first stage crystallization, which initiates at about 400°C (Fig. 8a), the $M(T)$ curve shows a minimum at about 420°C. The magnetic moment then increases with T, indicating that the separated metastable crystallites are ferromagnetic with a relatively high Curie temperature T_c in comparison to the amorphous phase. Extrapolating the curve to zero (indicated by A, see Fig. 8b), the T_c for the amorphous phase can be estimated to be about 440°C. With increasing temperature, the $M(T)$ curve shows another minimum (indicated by B) similar to that exhibited during the first-stage crystallization. The $M(T)$ curve in cooling process seems monotonic, but a small step near 250°C can be seen, suggesting a variety of crystalline phases in the annealed sample. The exchange interaction of magnetic atoms depends sensitively on the metalloid content in crystalline phases [15].

The effects of annealing on the magnetic properties are shown in Fig. 9 for a single film (90 nm). The heat treatment was made for 30 min successively at different temperatures up to 450°C. According to the DSC measurements (Fig. 8a), the sample remains amorphous up to 400°C, though it is possible that a structural relaxation could occur during the annealing, followed with an enhancement in short range ordering caused by an atomic cooperative process [9].

Before the annealing, the sample shows a coercive field H_c of 1.5 Oe along the easy axis and a magnetic anisotropy H_{aniso} of about 50 Oe (Fig. 9). In the amorphous state, the annealing-induced effect only shows a slight increase in H_c. Until 400°C it is no more than 2.5 Oe. The change of the anisotropic field, on the other hand, is pronounced. As can be followed in Fig. 9b, H_{anis} decreases quickly above 250°C and even falls to zero at 450°C. The phenomena can be attributed to the change of exchange reactions between magnetic atoms, possibly due to the atomic structure relaxation, which becomes particularly large near the crystallization temperature. Above 400°C, the sample begins to crystallize and as a result, H_c increases abruptly due to the pinning effect from crystalline particles. The annealing-induced effect on the saturation magnetization is not pronounced. It remains almost constant (680 emu/cm^3) up to the final crystallization temperature.

For sample series 1, the annealing effect is most marked for the thinnest samples (2 nm), except the sample of Ta/CoFeNiSiB/Ta. Even at 300°C, the H_c measured from the 2 nm samples with a Cu capping layer is enlarged by a factor of 6 to 7 (Fig. 10a and c). The result mirrors an additional effect possibly from thermally unstable interfaces due to the positive mixing heat mentioned above, which could induce an atomic rearrangement near the interface even at rather low annealing

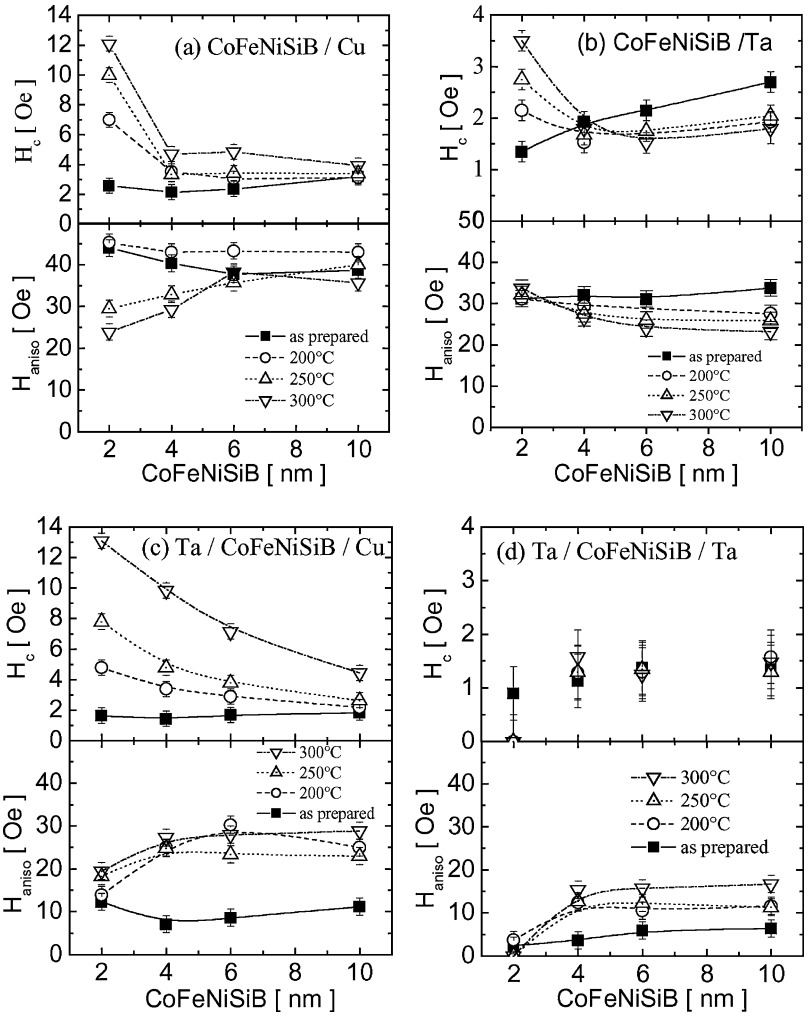

Figure 10 Effect of annealing on the magnetic anisotropy, including thickness dependence and interfacial influence from additional layers of Ta and Cu.

temperatures. For the thick samples the interfacial effect does not dominate and their annealing behavior is similar to the single film (Fig. 9). For the CoFeNiSiB/Ta and Ta/CoFeNiSiB/Ta samples, which already show a relatively large dead layer thickness due to interfacial mixing, the annealing effect below 300°C is insignificant (see Fig. 10b and d).

4. Conclusions

In summary, this paper presents the structural and magnetic properties of CoFeNi-based amorphous layers, and how they are affected by annealing and interfacial influences caused by additional layers of Cu and Ta. The samples which were prepared by magnetron-sputtering, showed typical amorphous structures with atomic short range ordering, a well-defined uniaxial anisotropy with a small coercive field of 1–2 Oe and a saturation magnetization of about 680 emu/cm^3. The excellent soft magnetic properties observed suggest that the CoFeNi-based amorphous materials are very promising for application in magnetoelectronic devices based on TMR junctions. The in-plane magnetic anisotropy was found to be dependent on sputtering geometry, showing two competing mechanisms. The first one arises from the stray field of the magnetron and causes a pair-ordering anisotropy of the magnetic atoms. The second one is due to an oblique incidence effect related to a topographical anisotropy of the film surface, which determines the orientation of local magnetic moment. The oblique incidence effect was dominant in the samples prepared with moving substrates and could be reduced by a Ta buffer layer due to decreased layer roughness. However, the interfacial mixing resulted in a limited magnetic dead layer in the samples.

Thermal analyses reveal that the amorphous state is stable up to 400°C, followed by a two-stage crystallization. The Curie temperature of the amorphous phase is estimated to be about 440°C. For the thinnest samples capped by a Cu layer, the annealing-induced effect becomes pronounced even at very low temperatures (<300°C), which can be attributed to rearrangement of the interfacial atoms due to the immiscibility of Cu and Co.

Acknowledgements

The authors would like thank Joachim Wecker and Manfred Rührig (Siemens AG Erlangen) for many helpful discussions. This work was supported by EU-project of "Tunnelsense" BE 97-4961 and by DFG-project of SA 337/9-1.

References

1. M. N. BAIBICH, J. M. BROTO, A. FERT, F. NGUYEN VAN DAU, F. PETROFF, P. ETIENNE, G. CREUZET, A. FRIEDRICH and J. CHAZELAS , *Phys. Rev. Lett.* **61** (1988) 2472.
2. J. S. MOODERA, L. R. KINDER, T. M. WONG and R. MESERVEY, *ibid.* **74**(16) (1995) 3273.
3. In Proceedings of the 4 th International Symposium on Metallic Multilayers (MML'01), 24–29 June 2001, Aachen, Germany; *J. Magn. Magn. Mat.* **240**(1–3) (2002).
4. R. C. O'HANDLEY, Modern Magnetic Materials Principles and Applications (Wiley-interscience, 1999).
5. R. R. GAREEV, S. S. ALIMPIEV, YU. V. BUGOSLAVSKII, S. M. NIKIFOROV, A. I. MASLOV, G. YU. SHUBNII and A. N. ZHERICHIN, *Acta Physica Polonica* **A 91** (1997) 321.
6. A. KÄUFLER, Y. LUO, K. SAMWER, G. GIERES, M. VIETH and J. WECKER, *J. Appl. Phys.* **91** (2002) 1701.
7. M. KOWALEWSKI, W. H. BUTLER, N. MOGHADAM, G. M. STOCKS, T. C. SCHULTHESS, K. J. SONG, J. R. THOMPSON, A. S. ARROTT, T. ZHU, J. DREWES, R. R. KATTI, M. T. MCCLURE and O. ESCORCIA, *ibid.* **87** (2000) 5732.
8. A. KÄUFLER Dissertation of University Göttingen (2002) .
9. Y. LUO, J. ZHAO and S. HUANG, *Acta Phys. Sin.* **31** (1983) 1256 and J. ZHAO, Y. LUO and S. HUANG, *Chinese Phys.* **3** (1983) 547.
10. H. FUJIMORI, "Amorphous Metallic Alloys," edited by F. E. Luborsky, Butterworths Monographs in Materials (1983) ch. **16** p. 300.
11. M. EßELING, Y. LUO and K. SAMWER, Magnetic and Structural Properties of CoFeHfO- films, submitted to *Appl. Phys. Lett.* (2003).
12. S. LICHTER and J. CHEN, *Phys. Rev. Lett.* **56** (1986) 1396.
13. S. G. MAYR, M. MOSKE and K. SAMWER, *Phys. Rev.* B **60** (1999) 16950.
14. D. C. PARKS, P. J. CHEN, W. F. EGELHOFF JR. and R. D. GOMEZ, *J. Appl. Phys.* **87** (2000) 3023.
15. H. Q. GUO, B. G. SHEN, D. M. LIN and S. T. PAN, *J. Mag. Mag. Mat.* **23** (1981) 156.
16. C. F. CONDE and A. CONDE, *Mater. Sci. Forum* **269–272** (1998) 719.